Hindawi
International Journal of Distributed Sensor Networks
Volume 2023, Article ID 9948725, 10 pages
https://doi.org/10.1155/2023/9948725

Research Article

Multiantenna Clustering Collaboration for WPCNs Based on Nonlinear EH

Lina Yuan,[1] **Huajun Chen**,[2] **Anran Zhou**,[3] **Rong Wang**,[4] **and Xianli Wen**[4]

[1]*School of Data Science, Tongren University, Tongren, China 554300*
[2]*School of Automation, Guangdong University of Technology, Guangzhou, China 510006*
[3]*College of Computer Science, Chengdu University, Chengdu, China 610106*
[4]*Engineering Technology Research Institute of Xinjiang Oilfield Company, Kelamayi, Xinjiang, China 834000*

Correspondence should be addressed to Lina Yuan; dsjyln@gztrc.edu.cn

Received 27 February 2023; Revised 11 September 2023; Accepted 25 October 2023; Published 14 November 2023

Academic Editor: Antonio Lazaro

This article considers a wireless-powered communication network (WPCN) composed of a multiantenna hybrid access point (HAP) based on nonlinear energy harvesting (EH). To improve some distant WDs' throughput performance, one of them is allowed to be selected as a cluster head (CH) to help transfer information from other cluster members (CMs). Nevertheless, the proposed clustering collaboration's performance is essentially restricted by the CH's energy-intensive consumption (EC), which requires to transfer every WDs' information, covering its own. In order to figure out the question, the HAP's energy beamforming (EB) capability with multiple antennas is utilized that can concentrate greater transmission power into the CH to equilibrate its EC to assist other WDs. To be specific, each WD's throughput performance is firstly derived under the proposed approach. A high-efficiency optimization algorithm for addressing cooperative optimization problem is put forward. In addition, the simulations are carried out in the actual network environment, and the results demonstrate that our proposed clustering collaboration with multiple antennas can validly enhance the WPCN's throughput fairness based on nonlinear EH.

1. Introduction

Wireless energy-constrained networks usually refer to the network whose nodes can only use storage energy such as small-capacity batteries for power supply due to the limitations of their size, location, and environment, such as wireless-powered communication networks (WPCNs) [1–4], wireless-powered sensor network (WPSN) [5, 6], wireless body area network [7], and a new type of wireless Internet of things network, for instance, smart transportation, smart medical treatment, and smart agriculture. In these networks, most wireless users are battery-powered. However, the limited capacity of batteries makes it difficult for them to work continuously for a long time, which has become the main bottleneck restricting their large-scale deployment. For example, in WPCN and WPSN, most sensors are deployed in unattended areas with harsh environment, which makes it difficult and costly to replace batteries. The use of disposable battery implantation has severely restricted the life cycle of wireless networks. In wireless body area network, wearable devices, especially the sensor devices implanted in the human body, have extremely limited power storage capacity due to the volume limitation, so it is unrealistic to extend the network life cycle by regularly replacing the device battery through frequent surgery. In [8], nonorthogonal multiple access- (NOMA-) assisted federated learning is studied, in which a group of terminal devices forms a NOMA cluster and sends their locally trained models to a cellular base station for model aggregation. Thus, how to improve the performance of network system while ensuring the energy supply of network nodes and extending the network life cycle has become a significant problem to be solved urgently in the design of wireless energy-constrained networks. In addition, how to provide

sustainable and steady power for wireless energy limited networks has become a new demand and challenge in the era of intelligent connection.

In order to work out the above-mentioned issues, academia and industry, on the one hand, lower the nodes' energy consumption (EC) and enhance the network energy efficiency and spectrum efficiency through the continuous development and evolution of advanced wireless communication technology (such as multiantenna technology and cooperative communication technology). On the other hand, the technology of energy harvesting (EH) in view of radio frequency (RF) signal is introduced to collect renewable energy or reusable energy from the surrounding environment to provide continuous and stable energy for network nodes. Further, combining wireless communication technology and EH technology based on RF signal, new technologies that are efficient and meet the needs of information and energy transmission have been proposed and studied successively.

Before 2015, the research on wireless EH only considered the linear EH model's application. Not until 2015 the nonlinear logic EH model was proposed, and both linear and nonlinear EH models began to be considered for exploration. For energy transformation efficiency, in the linear EH pattern, it is usually expressed by a constant. Therefore, [9] in 2016 pointed out that the energy transformation efficiency was a nonlinear variable, which was expressed by a polynomial function, and a heuristic EH model was proposed. However, the mathematical expressions of these two nonlinear EH models are complicated and difficult to analyze in many research problems. It is hard to obtain the studied problems' closed-form analytical results. In addition, in order to simplify the model, facilitate theoretical analysis, and depict the EH's nonlinear characteristics, the approximate nonlinear piecewise EH pattern was proposed in [10] in the same year. To describe the actual EH circuit's sensitive property, namely, the starting voltage, the modified logic EH model was proposed in 2017 in [11]. When the EH receiver's input power does not reach input voltage requirement, output power is zero, indicating that the EH circuit is still in the nonworking state. In the same year, because logical EH pattern and heuristic EH pattern are with the respect to mathematics not suitable for the complex problems' analysis and derivation, through data fitting, [12, 13], respectively, proposed quadratic polynomial EH model and fractional EH model for the problem under study. In 2018, in order to explore the limited sensitivity and nonlinear characteristics of far-field actual EH system, piecewise EH model I was proposed in [14].

Figure 1 illustrates a multiantenna cluster-based collaboration for WPCNs in view of nonlinear EH. The hybrid access point (HAP) with multiple antennas in WPCNs adopts wireless energy transfer to provide a cluster of distant WDs for energy and accept their data transfer. This might correspond to a real-world setting in WPSNs, in which the moving HAP is paused in its course to provide energy to a densely deployed cluster of transducers supervising a specific location. As with traditional WSNs, one of the WDs is designated as a cluster head (CH), which forwards other cluster members' (CMs') information to the HAP. The article's specific contribution is shown below.

(i) A multiantenna clustering collaboration approach is proposed in WPCNs, where one WD is specified as a CH to relay the other sensors' message. In view of the CH's high energy consumption in traditional cluster-based collaborative solutions, EB technology is applied in the HAP to equilibrate the WDs' diverse EC rates

(ii) Using the proposed collaborative approach, a cooptimization issue for the design of EB, the emission time distribution between HAP and WDs, and the CH's emission power distribution is developed for max-min throughput, which can be obtained between all WDs to enhance user fairness. A high-efficiency optimum solution algorithm is put forward for figuring out the nonconvex optimization issues

(iii) A numerical calculus is performed to investigate the effectual various system settings on the proposed approach's performance. Compared with other benchmark approaches, we find that the collaboration scheme can validly enhance throughput performance. In addition, when the cluster nearest to the cluster center is chosen as a CH, while the cluster location is close, the channel within the cluster is strong, and the amount number of cluster collaboration is medium, the proposed coordination mode is the most effective

The organization of the rest part in the article is as follows. Wireless EH models are introduced in Section 2. Section 3 illustrates the system pattern and proposes the multiantenna clustering collaboration approach based on nonlinear EH. Section 4 analyzes the per-WD throughput performance. The maximum-minimum throughput optimization issue is formulated and an optimal band-aid arithmetic is put forward in Section 5. Section 6 evaluates the proposed collaboration's performance employing simulations. In the end, Section 7 summarizes the full text.

2. Wireless EH Models

Wireless EH technology adopts radio frequency (RF) signals as EH sources. Compared with traditional natural EH sources (such as wind, solar, and lightning), wireless EH technology has been widely concerned by industry and academia because of its better controllability and stability. The existing wireless EH models for energy collectors (ECs) can be roughly separated into two categories: linear EH pattern and nonlinear EH pattern.

2.1. Linear EH Pattern. In the Linear EH model, the EC's output and input energy increase linearly, which is

$$f(x) = \eta x, \tag{1}$$

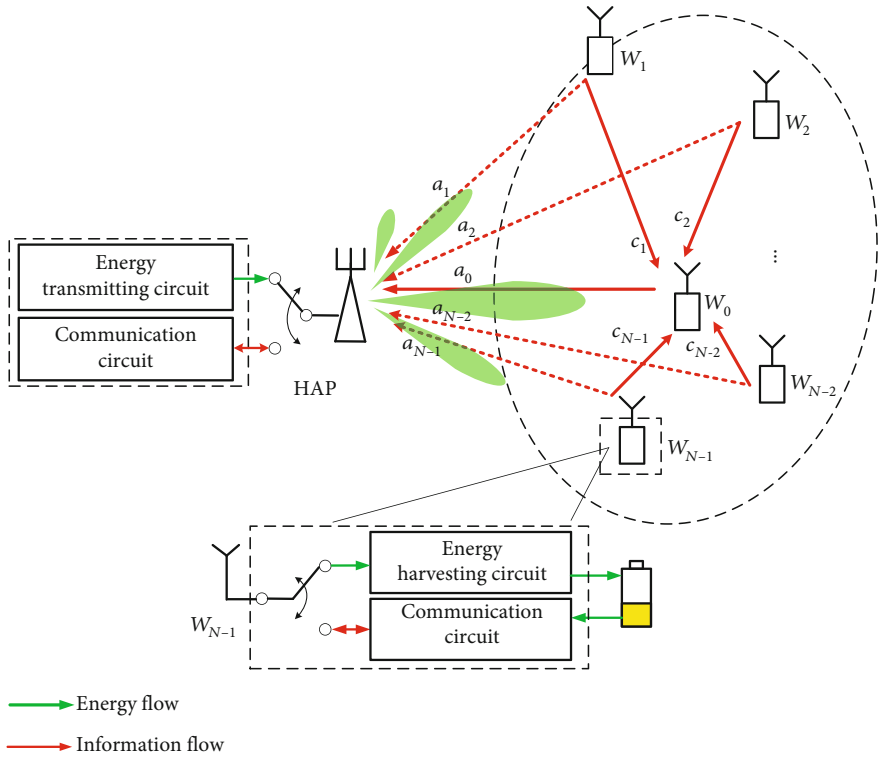

FIGURE 1: A diagram of the considered clustering collaboration for WPCNs, in which W_0 is the CH and the remaining $(N-1)$ WDs are CMs.

where η and x are the EC's transformation efficiency and input power, respectively. It can be seen from Equation (1) that η is independent of x. However, the actual EH circuit has nonlinear characteristics in the peer-to-peer energy transformation. To be specific, in the realistic EH circuit, while the input power arrives a certain level, the collected energy will reach saturation value and no longer increase linearly; that is, there is a maximum value of EH. Therefore, the application of linear models to practical EH circuits may lead to uncoordinated resource allocation. On the basis of linear EH models, researchers have proposed nonlinear EH models that can be roughly separated to five categories.

2.2. Nonlinear EH Pattern

2.2.1. The First Kind of Nonlinear EH Model (Case I). On the basis of the linear EH pattern, [14] proposes a new input-output relationship for the EC after testing dozens of practical ECs. Be associated with the linear EH pattern, case I is written as

$$f(x) = \eta(x)x, \tag{2}$$

where $\eta(x)$ is the EC's transformation efficiency and x is the input power from the EC. Different from the linear EH pattern, case I's energy transformation efficiency is not independent of the EC's input power constant. Here, the EC's transformation efficiency is given as the input power's function, which is

$$\eta(x) = \frac{p_2x^2 + p_1x + p_0}{q_3x^3 + q_2x^2 + q_1x + q_0}, \tag{3}$$

where p_0, p_1, p_2, q_0, q_1, q_2, and q_3 are obtained through curve fitting in [10–13]. For the EC of [10–15], the energy input and output relation of EC can be expressed as

$$f(x) = \eta(x)x = \frac{p_2x^3 + p_1x^2 + p_0x}{q_3x^3 + q_2x^2 + q_1x + q_0}. \tag{4}$$

As can be seen from Equation (4), within the input power's certain range, the EC's output power advances with input power. While the input power arrives a fixed value, the EC's input power reaches saturation state. According to Equation (4), while the input power advances, the nonlinear EH model's output power is virtually close to p_2/p_1. In addition, the linear EH pattern $f(x) = \eta x$ is regarded as obtained through disposing of Equation (4)'s highest terms in the numerator and denominator while x is tiny. This is the circumstance while the input power is tiny.

2.2.2. The Second Kind of Nonlinear EH Model (Case II). The actual parametric nonlinear EH model proposed by Boshkovska et al. [15] can describe the nonlinear characteristics of the actual EH circuit's peer-to-peer power conversion, as shown below:

$$\Phi = \frac{\left[\Psi_{\mathrm{ER}_n} - M_n\Omega_n\right]}{1 - \Omega_n}, \tag{5}$$

$$\Omega_n = \frac{1}{1 + \exp\left(a_n b_n\right)}, \tag{6}$$

$$\Psi_{\mathrm{ER}_n} = \frac{M_n}{1 + \exp\left(-a_n\left(P_{\mathrm{ER}_n} - b_n\right)\right)}, \tag{7}$$

where Ψ_{ER_n} is the conventional logic function relative to the RF power received by the user SU_n. The actual nonlinear EH model can describe the nonlinearity caused by hardware constraints by adjusting the parameters a_n, b_n, and M_n. In particular, M_n represents the collected maximum power at the EH user SU_n while the EH circuit is satiation. a_n and b_n are concerned with a minute EH circuit specification. These three parameters can be obtained through the given standard curve in view of a fixed EH circuit's measured data.

2.2.3. The Third Kind of Nonlinear EH Model (Case III). Case I and case II can describe the saturation of nonlinear models, but it is difficult to derive the mean value, the collected energy's probability density function, and the cumulative distribution function. On this basis, [14] proposed a simpler nonlinear EH model, which is written as

$$f(x) = \frac{ax + b}{x + c} - \frac{b}{c}, \tag{8}$$

where the parameters a, b, and c are invariable regulated through fitting the standard curve. The term b/c is summed to satisfy the case that the output power is zero while the EC's input power is small. In addition, similar to case I and case II, the EH model described in Equation (6) is more able to describe the nonlinearity and saturation of EH by the EC than the linear EH model. However, compared with case I and case II, the nonlinear EH model expressed in Equation (6) (case III) is simpler to operate, and it is easier to deal with the mean derivation.

2.2.4. The Fourth Kind of Nonlinear EH Model (Case IV). There are nonlinear components, for example, diodes in the EH circuit, so the output energy $p_{\mathrm{out}} = \Theta(p_{\mathrm{in}})$ of the EC has a nonlinear relationship with the input energy p_{in} of the EC. And this nonlinear function must meet the below characteristics:

(i) While p_{in} is less than the EC's threshold of sensitivity p_0, define $p_{\mathrm{out}} = \Theta(p_{\mathrm{in}}) = 0$

(ii) $\Theta(p_{\mathrm{in}})$ is about increasing function

(iii) With the increase of p_{in}, the conversion efficiency $\Theta(p_{\mathrm{in}})/p_{\mathrm{in}}$ of the EC will gradually increase until it arrives the maximum value and then decrease

(iv) For all p_{in} of $\Theta(p_{\mathrm{in}}) \le P_{\max}$, where $P_{\max}$ is the maximum energy collected while the EH circuit arrives saturation

Based on characteristics (i)-(iv), the curve of the relation formula should be an S shaped curve. In order to meet this feature, a logical model is put forward in [16], but [15]'s model does not meet the sensitivity feature (i). To solve this problem, [17] modifies the model proposed in [15], which can be expressed as

$$\Theta(p_{\mathrm{in}}) = \left[\frac{P_{\max}}{\exp\left(-\tau p_0 + \nu\right)}\left(\frac{1 + \exp\left(-\tau p_0 + \nu\right)}{1 + \exp\left(-\tau p_{\mathrm{in}} + \nu\right)} - 1\right)\right]^{+}. \tag{9}$$

In view of the above equation, the collected energy at the EH equipment i is $\Theta(1 - \beta_{i,m} p_m |g_{i,m}^H v_m|^2)$. All the features for (i)-(iv) can be verified from the above equation. Also, the parameters' (τ's and ν's) steepness can control functions, i.e., in equation (9).

2.2.5. The Fifth Kind of Nonlinear EH Model (Case V). The collected energy through the EH circuit is sculptured as

$$P_{\mathrm{har}}^{(n)} \equiv P_{\mathrm{har}}^{(n)}\left(P_R^{(n)}\right) = p\left(P_R^{(n)}\right), \tag{10}$$

Here,

$$p(x)\Delta = \begin{cases} 0, & x \in \left[0, P_{\mathrm{in}}^{\mathrm{sen}}\right], \\ \eta(x) * x, & x \in \left[P_{\mathrm{in}}^{\mathrm{sen}}, P_{\mathrm{in}}^{\mathrm{sat}}\right], \\ \eta\left(P_{\mathrm{in}}^{\mathrm{sat}}\right) * P_{\mathrm{in}}^{\mathrm{sat}}, & x \in \left[P_{\mathrm{in}}^{\mathrm{sat}}, \infty\right]. \end{cases} \tag{11}$$

Function $\eta(P_R^n)$ denotes the function of the input power energy conversion efficiency. Define $P_{\mathrm{in}}\Delta = [P_{\mathrm{in}}^{\mathrm{sen}}, P_{\mathrm{in}}^{\mathrm{sat}}]$. $P_{\mathrm{in}}^{\mathrm{sen}}$ represents the sensitivity of the EC. For every input power less than the sensitivity, the energy harvested through the EC is 0. When $x \le P_{\mathrm{in}}^{\mathrm{sen}}$, $P(x) = 0$. Let $P_{\mathrm{in}}^{\mathrm{sat}}$ denote the saturation value of the energy collected through the EC, after which the collected energy is all constant.

(i) EC's function harvested energy P: assume $R_+ \longrightarrow R_+$

(ii) Nondecreasing

(iii) Continuity

The experiments prove that the above assumption is consistent with the EH curve in the EH circuit in the prior art. The energy conversion efficiency is written as

$$\eta(x) = \omega_0 + \sum_{i=1}^{W} \omega_i (10\log_{10}(x)), \tag{12}$$

where x is in units of milliwatt, W is the fitting polynomial's order in units of dBm, and $\{\omega_i\}_{i=0}^{W}$ is the polynomial's coefficient. For the model, the polynomial of the fitting function's order is $W = 10$ and $W = 12$, respectively. Furthermore, $P_{\mathrm{in}} = [10^{-4.25}, 10^{1.6}]$ and $P_{\mathrm{in}} = [10^{-1.2}, 10]$ are all in units of milliwatt.

3. System Model

3.1. Channel Model. A WPCN is considered as demonstrated in Figure 1, which is composed of one HAP and N WDs.

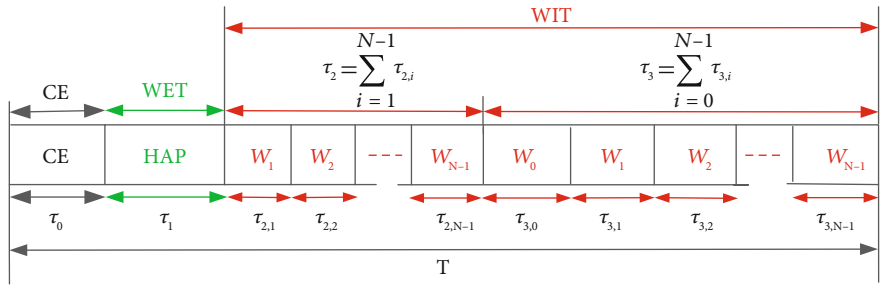

Figure 2: Our suggested clustering collaboration protocol for WPCNs.

The HAP has power supply stablility and is installed with M-antenna ($N >> M$ in practice). Every sensor with one antenna has a built-in battery to save wireless collected energy from the HAP. To be specific, the HAP multicasts radio energy to the sensors and accepts the sensors' wireless information transfer (WIT). The HAP and each WD operate in the identical frequency band and carry out a time-division duplex circuit to realize the separation of energy and information transfer.

One of the sensors is chosen as the CH to assist transferring other CMs' WIT in this paper. Without loss of generality, make W_0 and $W_1, \cdots, W_{N-1}$ index as the CH and CMs, respectively. Suppose all channels are mutual independence, keeping to quasistatic flat-fading; in this way, the coefficients of all channels hold constant for transferring time per block, expressed as T; however, it can be different by block. Make $\mathbf{a}_i \in \mathscr{C}^{M\times 1}$ represent the channel coefficient's vector between the HAP and W_i, where $\mathbf{a}_i \sim \mathscr{CN}(\mathbf{0}, \sigma_i^2\mathbf{I})$ and σ_i^2, $i = 0, 1, \cdots, N-1$, represents the average channel gain. Besides, $c_j \sim \mathscr{CN}(0, \delta_j^2)$ represents path coefficient between the CH and the j-th CM ($j = 1, \cdots, N-1$). Here, $h_i \triangleq |\mathbf{a}_i|^2$ and $g_i \triangleq |c_i|^2$ represent the relevant channel gains, in which $|\cdot|$ represents the 2-norm operator.

3.2. Clustering Collaborative Protocol in View of Nonlinear EH. Figure 2 illustrates the run of our proposed clustering cooperation protocol based on nonlinear EH in a transport time block. At the start of a transfer block, it spends a constant duration τ_0 on acting channel estimation (CE). At the CE's section, the WDs alternate order to radio their pilot signals, making the HAP and the CH to know c_i ($i = 1, \cdots, N-1$) and $\mathbf{a}_i$ ($i = 0, 1, \cdots, N-1$), separately. After that, the CH transmits the HAP c_i's estimation, making the HAP have all the information about CSI in the mesh.

After the CE's phase, three phases are run for the system. During the first stage, time duration is τ_1, and the HAP multicasts wireless energy with a settled transmitting power of P. During the next two stages with $T - \tau_0 - \tau_1$, the N sensors transfer their separate nessages to the HAP adopting their acquired energy. To be specific, firstly, the $(N-1)$ CMs transfer sequentially to the CH, in which the i-th CM transfers at the time of $\tau_{2,i}$ ($i = 1, \cdots, N-1$). During the third phase, the CH transfers the $(N-1)$ CMs' decoded information to the HAP in conjunction with its own information. Make $\tau_{3,i} (i = 0, 1, \cdots, N-1)$ as the time spent on transferring the i-th WD's message. Obviously, time allocations meet the below inequations

$$\tau_0 + \tau_1 + \sum_{i=1}^{N-1} \tau_{2,i} + \sum_{i=0}^{N-1} \tau_{3,i} \le T. \tag{13}$$

Note that τ_0 is a given coefficient. Without lossing generality, this article supposes $T = 1$. On account of the global CSI's knowledge, the HAP can figure out the optimum time allocation, which is thus broadcast to each WD so that time-switching circuits are kept by them with synchronizing for either information and energy transmission. The next part will deduce the proposed collaborative protocol's throughput performance and formulate the optimization problem of maximum-minimum (max-min) throughput.

4. The Analysis of Per-WD Throughput

4.1. Phase I: Energy Transmission. Note that the CH becomes the network's performance bottleneck, because the CH requires to transfer a total of N messages, which will consume obviously more energy than the other CMs. During the first stage of τ_1, the HAP transfers $\mathbf{w}(t) \in C^{M\times 1}$ stochastic energy signals on the M-antenna, in which the HAP's transmitting power is influenced on

$$E\left[|\mathbf{w}(t)|^2\right] = \mathrm{tr}\left(E\left\{\mathbf{w}(t)\mathbf{w}(t)^H\right\}\right) \triangleq \mathrm{tr}(\mathbf{Q}) \le P, \tag{14}$$

where $\mathrm{tr}(\cdot)$, $(\cdot)^H$, and $\mathbf{Q} \ge \mathbf{0}$ express a matrix's trace, the complex conjugation operator, and the EB matrix, respectively. The receiver noise power is denoted by $n_i^{(1)}(t)$, and thus, the received energy signal by the i-th WD can be written as

$$y_i^{(1)}(t) = \mathbf{a}_i^T\mathbf{w}(t) + n_i^{(1)}(t), i = 0, \cdots, N-1, \tag{15}$$

With ignoring interference power, the obtained energy through sensors is indicated as [7]

$$E_i^{\mathrm{CH_{NL}}} = \frac{(M/(1+\exp(-a(\tau_1(\mathrm{tr}(A_iQ)) - b)))) - (M/(1+\exp(ab)))}{1 - (1/(1+\exp(ab)))} \triangleq \psi(\tau_1 \mathrm{tr}(\boldsymbol{A}_i\mathbf{Q})), i = 0, \cdots, N-1. \tag{16}$$

Here, $\mathbf{A}_i \triangleq \mathbf{a}_i\mathbf{a}_i^H$, $\psi(x_i) = (\beta(x_i) - M\Omega)/(1-\Omega)$, $\Omega = 1/(1+\exp(ab))$, $\beta(x_i) = M/(1+\exp(-a(x_i-b)))$, $E_i^{\mathrm{CH_{NL}}}$ is an input power's typical Sigmoid function, Ω is used to ensure this model's zero input and zero output and keep the quantity constant, M is the circuit's maximum output power at saturation, which is also a constant, and a and b are related to the impedance, capacitance, and conduction voltage of the diode in the circuit, keeping their values constant.

4.2. Phase II: Intracluster Transfer. Suppose in the second phase the CMs will consume the collected energy to the CH. Then, the i-th CM's transmitting power is

$$P_{2,i}^{\mathrm{CH_{NL}}} = \frac{E_i^{\mathrm{CH_{NL}}}}{\tau_{2,i}} \triangleq \frac{\psi(\tau_1 \mathrm{tr}(\boldsymbol{A}_i\boldsymbol{Q}))}{\tau_{2,i}}, i = 1, \cdots, N-1. \quad (17)$$

The i-th WD's baseband signal transferred in the second stage and the receiver noise with power are denoted by $s_i^{(2)}(t)$ with $E[|s_i^{(2)}(t)|^2] = 1$ and $n_i^{(2)}(t)$ with $E[|n_i^{(2)}(t)|^2] = N_0$, respectively. Then, the signal received at the CH is

$$y_{0,i}^{(2)}(t) = c_i\sqrt{P_{2,i}^{\mathrm{CH_{NL}}}}s_i^{(2)}(t) + n_i^{(2)}(t). \quad (18)$$

Thus, the i-th CM's messages are decoded through the CH with a fixed rate by

$$R_i^{(2)} = \tau_{2,i}\log_2\left(1 + \frac{g_i P_{2,i}^{\mathrm{CH_{NL}}}}{N_0}\right), i = 1, \cdots, N-1. \quad (19)$$

In the meantime, the HAP can eavesdrop on the CMs' transfer as well, so that it receives within the i-th CM's transfer

$$\mathbf{y}_{H,i}^{(2)}(t) = \mathbf{a}_i\sqrt{P_{2,i}^{\mathrm{CH_{NL}}}}s_i^{(2)}(t) + \mathbf{n}_{H,i}^{(2)}(t), i = 1, \cdots, N-1, \quad (20)$$

where $\mathbf{n}_{H,i}^{(2)}(t) \sim \mathcal{CN}(\mathbf{0}, N_0\mathbf{I})$.

For the sake of simplicity, the decoding's EC is ignored, and the data transmission's EC is only considered. However, by introducing an unchanging circuit power term, our proposed approach is readily expanded when the decoding EC is nonzero.

4.3. Phase III: Cluster-to-HAP Transfer. When completing to decode the CMs' information, the CH sends the $(N-1)$ CMs' information to the HAP one by one, along with its own information. The CH's baseband signal and the i-th CM's reencoded baseband signal transmitted in the third stage are denoted by $s_0^{(3)}(t)$ and $s_i^{(3)}(t)$, respectively. In addition, suppose the power adopted to transfer the i-th WD's information is expressed as $P_{3,i}^{\mathrm{CH_{NL}}}$ and $E[|s_i^{(3)}(t)|^2] = 1$, $i = 0, \cdots, N-1$. Then, at the HAP, the i-th WD information's received signal is

$$\mathbf{y}_i^{(3)}(t) = \mathbf{a}_0\sqrt{P_{3,i}^{\mathrm{CH_{NL}}}}s_i^{(3)}(t) + \mathbf{n}_i^{(3)}(t), i = 0, 1, \cdots, N-1. \quad (21)$$

The aggregated EC through the CH is upper bound on the energy it harvests E_0, i.e.,

$$\sum_{i=0}^{N-1}\tau_{3,i}P_{3,i}^{\mathrm{CH_{NL}}} \le \psi(\tau_1\mathrm{tr}(A_0Q)). \quad (22)$$

Suppose that maximal ratio combining (MRC) is adopted by the HAP to maximize the receive signal-to-noise power ratio (SNR), in which the i-th WD's combiner output SNR is

$$\gamma_i^{(3)} = \frac{|\mathbf{a}_0|^2 P_{3,i}^{\mathrm{CH_{NL}}}}{N_0} = \frac{h_0 P_{3,i}^{\mathrm{CH_{NL}}}}{N_0}, i = 0, \cdots, N-1. \quad (23)$$

The time distribution and transmitting power are denoted as $\tau = [\tau_1, \tau_{2,1}, \cdots, \tau_{2,N-1}, \tau_{3,0}, \tau_{3,1}, \cdots, \tau_{3,N-1}]'$ and $\mathbf{P}^{\mathrm{CH_{NL}}} = [P_{3,0}^{\mathrm{CH_{NL}}}, P_{3,1}^{\mathrm{CH_{NL}}}, \cdots, P_{3,N-1}^{\mathrm{CH_{NL}}}]'$. Then, the CH's throughput at the HAP is

$$R_0^{\mathrm{CH_{NL}}}(\tau, \mathbf{P}^{\mathrm{CH_{NL}}}) = \tau_{3,0}\log_2\left(1 + \frac{h_0 P_{3,0}^{\mathrm{CH_{NL}}}}{N_0}\right). \quad (24)$$

However, the second and third stages can receive every CM's information. On this occasion, the HAP could code-code every CM's information at a given rate across two stages by

$$R_i^{\mathrm{CH_{NL}}}(\tau, \mathbf{P}^{\mathrm{CH_{NL}}}, \mathbf{Q}) = \min\left\{R_i^{(2)}(\tau, \mathbf{Q}), V_i^{(2)}(\tau, \mathbf{Q}) + V_i^{(3)}(\tau, \mathbf{P}^{\mathrm{CH_{NL}}})\right\}, \quad i = 1, \cdots, N-1, \quad (25)$$

where (19) gives $R_i^{(2)}(\tau, \mathbf{Q})$ and $V_i^{(2)}(\tau, \mathbf{Q})$ expresses the information extracted from the received signal by the HAP, where an optimal MRC receiver is used in (18) (during the second phase) that is written as

$$V_i^{(2)}(\tau, \mathbf{Q}) = \tau_{2,i}\log_2\left(1 + \frac{\psi(\tau_1\mathrm{tr}(A_iQ))g_i}{\tau_{2,i}}\right). \quad (26)$$

$V_i^{(3)}(\tau, \mathbf{P}^{\mathrm{CH_{NL}}}, \mathbf{Q})$ expresses the transmissions' attainable rates from the CH to the HAP, which is

$$V_i^{(3)}(\tau, \mathbf{P}^{\mathrm{CH_{NL}}}) = \tau_{3,i}\log_2\left(1 + \frac{h_0 P_{3,i}^{\mathrm{CH_{NL}}}}{N_0}\right). \quad (27)$$

The max-min throughput is a WPCN's significant performance index, defined as

$$S^{\mathrm{CH_{NL}}} = \min_{0\le i\le N-1} R_i^{\mathrm{CH_{NL}}}. \quad (28)$$

5. Maximum and Minimum Throughput Optimization

5.1. Problem Formulation. This part maximizes all WDs' max-min throughput within each block, through cooptimizing

EB $\mathbf{Q}$ and the allocation of time τ and transmitting power $\mathbf{P}^{\mathrm{CH_{NL}}}$, that is,

$$\begin{aligned}(P1):\ &\max_{\tau,\mathbf{P}^{\mathrm{CH_{NL}}},\mathbf{Q}} \quad S=\min_{0\le i\le N-1} R_i\left(\tau,\mathbf{P}^{\mathrm{CH_{NL}}},\mathbf{Q}\right)\\ &\text{s.t.}\quad (1)\text{ and }(10),\\ &\tau_1\ge 0,\tau_{2,i}\ge 0,i=1,\cdots,N-1,\\ &\tau_{3,i}\ge 0,P_{3,i}^{\mathrm{CH_{NL}}}\ge 0,i=0,1,\cdots,N-1,\\ &\mathrm{tr}(\mathbf{Q})\le P,\mathbf{Q}\ge\mathbf{0},\tau\ge\mathbf{0}.\end{aligned}\tag{29}$$

We introduce a variant $\bar{S}^{\mathrm{CH_{NL}}}$ and equivalently convert problem (P1) to its inscription form:

$$\begin{aligned}(P2):\ &\max_{\tau,\mathbf{P}^{\mathrm{CH_{NL}}},\mathbf{Q},\bar{S}^{\mathrm{CH_{NL}}}} \bar{S}^{\mathrm{CH_{NL}}}\\ &\text{s.t.}\quad (1)\text{ and }(10),\\ &R_0\left(\tau,\mathbf{P}^{\mathrm{CH_{NL}}}\right)\ge\bar{S}^{\mathrm{CH_{NL}}},\\ &V_i^{(2)}(\tau,\mathbf{Q})+V_i^{(3)}\left(\tau,\mathbf{P}^{\mathrm{CH_{NL}}}\right)\ge\bar{S}^{\mathrm{CH_{NL}}},\\ &R_i^{(2)}(\tau,\mathbf{Q})\ge\bar{S}^{\mathrm{CH_{NL}}},i=1,\cdots,N-1,\\ &\mathrm{tr}(\mathbf{Q})\le P,\mathbf{Q}\ge\mathbf{0},\tau\ge\mathbf{0}.\end{aligned}\tag{30}$$

Because of user collaboration and beamforming design, $R_i^{(2)}(\tau,\mathbf{Q})$ and $V_i^{(2)}(\tau,\mathbf{Q})$), i.e., the throughput within intracluster communication, are concave functions. Meanwhile, $R_0(\tau,\mathbf{P}^{\mathrm{CH_{NL}}})$ and $V_i^{(3)}(\tau,\mathbf{P}^{\mathrm{CH_{NL}}})$, i.e., the data rates within cluster-to-HAP communication, are also not concave functions. In addition, the (10)'s left hand side is not convex as well. Therefore, the (P2)'s present form is a nonconvex issue and lacks efficient optimization algorithm. The algorithm for optimal solution (P2) will be proposed in the next subsection.

5.2. (P2) Optimization Algorithm. Above all, define $\mathbf{W}\triangleq\tau_1\mathbf{Q}\ge\mathbf{0}$. With the total transmitted power constraint is at (14), which we have

$$\mathrm{tr}(\mathbf{W})=\mathrm{tr}(\tau_1\mathbf{Q})\le\tau_1 P.\tag{31}$$

Therefore, the variables are changed as

$$z_i\triangleq\tau_1\mathrm{tr}(\mathbf{A}_i\mathbf{Q})=\mathrm{tr}(\mathbf{A}_i\mathbf{W}),i=0,\cdots,N-1.\tag{32}$$

Therefore, $R_i^{(2)}(\tau,\mathbf{Q})$ and $V_i^{(2)}(\tau,\mathbf{Q})$ in (19) and (26) are represented as the functions of τ and $\mathbf{z}=[z_1,\cdots,z_{N-1}]$:

$$\begin{aligned}R_i^{(2)}(\tau,\mathbf{z})&=\tau_{2,i}\log_2\left(1+\bar{\rho}_i\frac{z_i}{\tau_{2,i}}\right),i=1,\cdots,N-1,\\ V_i^{(2)}(\tau,\mathbf{z})&=\tau_{2,i}\log_2\left(1+\rho_i\frac{z_i}{\tau_{2,i}}\right),i=1,\cdots,N-1,\end{aligned}\tag{33}$$

in which $\bar{\rho}_i\triangleq g_i/N_0$ and $\rho_i\triangleq h_i/N_0$ are parameters.

Then, define $\theta_{3,i}\triangleq\tau_{3,i}P_{3,i}^{\mathrm{CH_{NL}}}$ $(i=0,1,\cdots,N-1)$; thus, $R_0(\tau,\mathbf{P}^{\mathrm{CH_{NL}}})$ and $V_i^{(3)}(\tau,\mathbf{P}^{\mathrm{CH_{NL}}})$ in (24) and (27) is reformulated as the functions of τ and $\theta=[\theta_{3,0},\cdots,\theta_{3,N-1}]$, i.e.,

$$\begin{aligned}R_0(\tau,\theta)&=\tau_{3,0}\log_2\left(1+\rho_0\frac{\theta_{3,0}}{\tau_{3,0}}\right),\\ V_i^{(3)}(\tau,\theta)&=\tau_{3,i}\log_2\left(1+\rho_0\frac{\theta_{3,i}}{\tau_{3,i}}\right),i=1,\cdots,N-1,\end{aligned}\tag{34}$$

where $\rho_0\triangleq h_0/N_0$. Therefore, given in (10) of power constraint is rerepresented as again

$$\sum_{i=0}^{N-1}\theta_{3,i}\le z_0.\tag{35}$$

Thus, (29) is converted into the same question as follows:

$$\begin{aligned}(P3):\ &\max_{\tau\ge\mathbf{0},\theta,\mathbf{z},\bar{S}^{CH_{NL}},\mathbf{W}\ge\mathbf{0}} \bar{S}^{\mathrm{CH_{NL}}}\\ &\text{s.t.}\quad R_0(\tau,\theta)\ge\bar{S}^{\mathrm{CH_{NL}}},\\ &V_i^{(2)}(\tau,\mathbf{z})+V_i^{(3)}(\tau,\theta)\ge\bar{S}^{\mathrm{CH_{NL}}},\\ &R_i^{(2)}(\tau,\mathbf{z})\ge\bar{S}^{\mathrm{CH_{NL}}},i=1,\cdots,N-1,\\ &\tau_0+\tau_1+\sum_{i=1}^{N-1}\tau_{2,i}+\sum_{i=0}^{N-1}\tau_{3,i}\le 1,\\ &z_i=\mathrm{tr}(\mathbf{A}_i\mathbf{W}),i=0,1,\cdots,N-1,\\ &\sum_{i=0}^{N-1}\theta_{3,i}\le z_0,\mathrm{tr}(\mathbf{W})\le\tau_1 P.\end{aligned}\tag{36}$$

From [18, 19], (P1)'s and (P3)'s optimal solution can be easily obtained.

6. Simulation Result Analysis

This part assesses our proposed collaborative approach's performance. In the simulations below, suppose that the HAP's transmitted power $P=3$ watts (W), energy collecting efficiency $\eta=0.51$ (please see the detailed product specifications on the website of Powercast Co. (http://www.powercastco.com)), the quantity of HAP antennas $M=5$, the antenna gain $G_A=2$, the carrier frequency $f_c=915$ MHz, the path-loss factor $\alpha=3$, and the interference power $N_0=10^{-10}$ W for all receivers' bandwidth. The average channel gain between every two sensors (HAP or one WD) keeps to a path-loss pattern. For example, make $d_{H,i}$ as the distance between the HAP and the i-th WD, and then, the mean channel gain $\delta_i^2=G_A((3\times10^8)/4\pi d_{H,i}f_c)^\alpha$. In addition, 15 WDs are uniform distribution in a circle of radius r meters (m), and the circle's center is d m away from the HAP. Every point in the graphs is an individual WD location with an average of 20 [1].

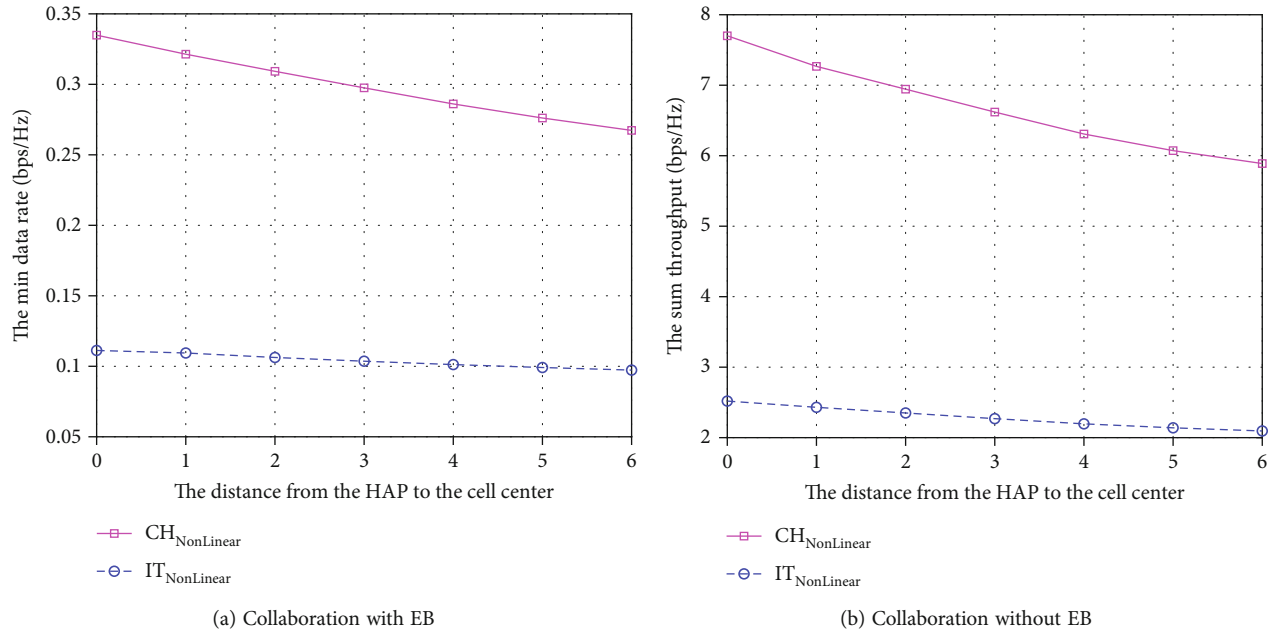

(a) Collaboration with EB (b) Collaboration without EB

FIGURE 3: The effect of CH selection on max-min throughput when $d = 6$ m. EB technology is used in HAP in (a), but not in (b).

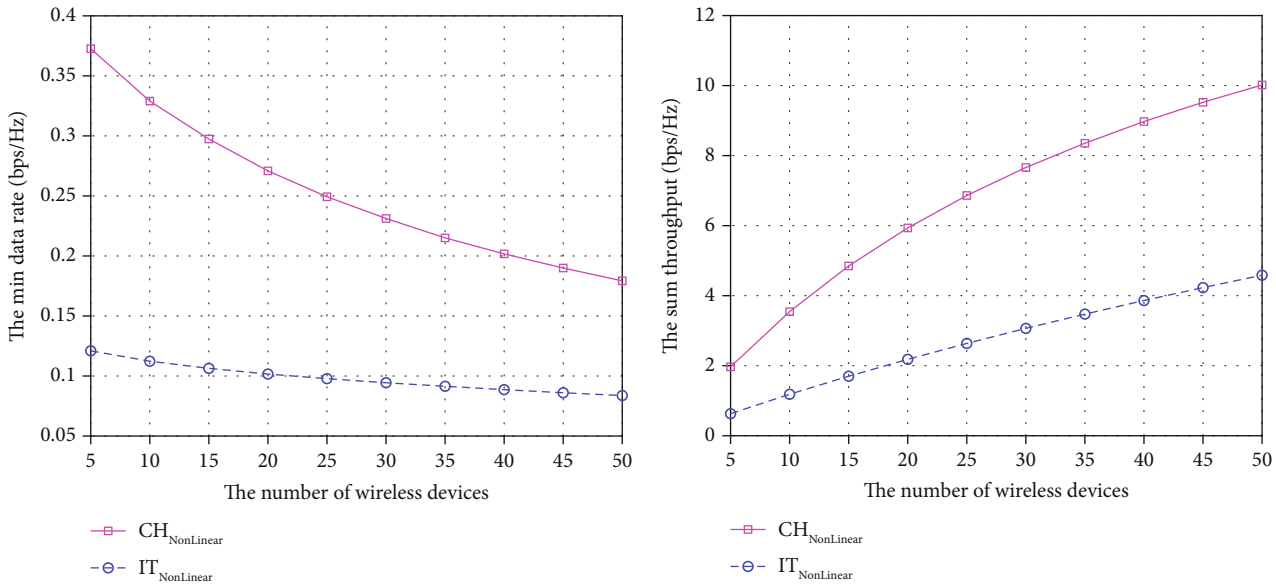

(a) Collaboration with EB (b) Collaboration without EB

FIGURE 4: The influence on CH selection on maximum-minimum throughput when $r = 3$ m. EB technology is used in HAP in (a), but not in (b).

Figure 3 examines cluster-to-HAP information links' effect on the total throughput's performance through setting $r = 3$ and changing d. We can observe from Figure 3 that the proposed collaborative approach gains significant performance advantage over the benchmark method. However, when d is further increased, very low data rates of both schemes are achieved because the energy signal dramatically attenuates over distance. The simulation results demonstrate that the collaborative approach's effective working scope under consideration is essentially confined by the relatively low energy transfer efficiency. As a matter of fact, WPC is only available if the power does not travel very far, which allows the WDs to gather enough power to transmit information. In a practical applications, the performance can be enhanced in several ways, for example, augmenting the number of HAP antennas, optimizing the routing for moving HAP, or adding the HAP's transmitting power.

In Figure 4, throughput performance's stability is evaluated as the number of WDs N is increased from 5 to 50 by setting $d = 6$ m and $r = 3$ m. Figure 4(a) shows that the

maximum-minimum throughput of both approaches lessens with N. The worst-performing WD lessens throughput due to the shorter average transfer time per sensor. Specially, as N increases from 35 to 50, the lessen in maximum-minimum throughput is modest. However, Figure 4(b) shows that the total throughput adds with N, although the throughput per WD may lower. This manifests that there is a trade-off between the throughput per WD and the total network. Even so, we can still become conscious of the proposed approach's important performance improvement over the benchmark method, while the network is big (for example, N equals 30).

7. Conclusions

In this article, a clustering collaborative approach is proposed for WPCNs based on nonlinear EH, in which one sensor is specified as a CH to help other WDs' propagation. An efficient algorithm is put forward to reach the optimal maximum-minimum throughput among the sensors, through cooptimizing the design of EB, the emission time distribution among the HAP and sensors, and the CH's emission power distribution. A large number of simulations in real mesh settings demonstrated that our suggested approach might remarkably advance user fairness and spectral efficiency, compared with nontrivial benchmark approaches.

Data Availability

The data in the paper can be obtained from corresponding authors.

Conflicts of Interest

The authors declared no potential conflicts of interest with respect to the research, authorship, and/or publication of this article.

Acknowledgments

This research was supported by the Doctoral Talent Project of Tongren Science and Technology Bureau (No. [2020]124), Doctoral Research Project of Tongren University (trxyDH2003), Basic Research Program of Guizhou Province (ZK[2021] General 299), Natural Science Foundation Fund Project in Guangxi of China under Grant 2021GXNSFBA220003, Doctoral Scientific Research Foundation of Yulin Normal University (No. G2019ZK44), and Science and Technology Planning Project of Guizhou Province ([2020]1Y260).

References

[1] S. Bi, C. K. Ho, and R. Zhang, "Wireless powered communication: opportunities and challenges," *IEEE Communications Magazine*, vol. 53, no. 4, pp. 117–125, 2015.

[2] S. Bi, Y. Zeng, and R. Zhang, "Wireless powered communication networks: an overview," *IEEE Communications Magazine*, vol. 23, no. 2, pp. 1284–1536, 2016.

[3] L. Yuan, H. Chen, and J. Gong, "Interactive communication with clustering collaboration for wireless powered communication networks," *International Journal of Distributed Sensor Networks*, vol. 18, no. 2, Article ID 155014772110699, 2022.

[4] L. Yuan, W. Zhang, J. Liang, and A. Zhou, "Nonlinear energy harvesting and clustering cooperation in WPCNs," *Wireless Personal Communication*, vol. 130, no. 2, pp. 1215–1230, 2023.

[5] N. Mazloomi, M. Gholipour, and A. Zaretalab, "Efficient configuration for multi-objective QoS optimization in wireless sensor network," *Ad Hoc Networks*, vol. 125, p. 102730, 2022.

[6] L. Yuan, H. Chen, and J. Gong, "Throughput optimization of multi-hop and multi-path cooperation in WPSNs with hardware noises," *International Journal of Distributed Sensor Networks*, vol. 17, no. 6, Article ID 15501477211024838, 2022.

[7] B. Cornet, H. Fang, H. Ngo, E. W. Boyer, and H. Wang, "An overview of wireless body area networks for mobile health applications," *IEEE Network*, vol. 36, no. 1, pp. 76–82, 2022.

[8] Y. Wu, Y. Song, T. Wang, L. Qian, and T. Q. S. Quek, "Non-orthogonal multiple access assisted federated learning via wireless power transfer: a cost-efficient approach," *IEEE Transactions on Communications*, vol. 70, no. 4, pp. 2853–2869, 2022.

[9] Y. Chen, K. T. Sabnis, and R. A. AbdAlhameed, "New formula for conversion efficiency of RF EH and its wireless applications," *IEEE Transactions on Vehicular Technology*, vol. 65, no. 11, pp. 9410–9414, 2016.

[10] Y. Dong, M. Hossain, and J. Cheng, "Performance of wireless powered amplify and forward relaying over Nakagamim fading channels with nonlinear energy harvester," *IEEE Communications Letters*, vol. 20, no. 4, pp. 672–675, 2016.

[11] Z. Chu, P. Xiao, D. Mi et al., "Wireless-powered intelligent radio environment with nonlinear energy harvesting," *IEEE internet of things journal*, vol. 9, no. 18, pp. 18130–18141, 2022.

[12] X. Xu, A. Ozcelikkale, and T. McKelvey, "Simultaneous information and power transfer under a non-linear RF energy harvesting model," in *Proceedings of 2017 IEEE International Conference on Communications Workshops (ICC Workshops)*, pp. 179–184, Paris, France, 2017.

[13] Y. Chen, N. Zhao, and M. S. Alouini, "Wireless energy harvesting using signals from multiple fading channels," *IEEE Transactions on Wireless Communication*, vol. 65, no. 11, pp. 5027–5039, 2017.

[14] P. N. Alevizos and A. Bletsas, "Sensitive and nonlinear far-field RF energy harvesting in wireless communications," *IEEE Transactions on Wireless Communication*, vol. 17, no. 6, pp. 3670–3685, 2018.

[15] E. Boshkovska, D. W. K. Ng, N. Zlatanov, and R. Schober, "Practical non-linear energy harvesting model and resource allocation for SWIPT systems," *IEEE Communications Letters*, vol. 19, no. 12, pp. 2082–2085, 2015.

[16] J. Zhang and G. Pan, "Outage analysis of wireless-powered relaying MIMO systems with non-linear energy harvesters and imperfect CSI," *IEEE Access*, vol. 4, pp. 7046–7053, 2016.

[17] S. Wang, M. Xia, K. Huang, and Y. C. Wu, "Wirelessly powered two-way communication with nonlinear energy harvesting model: rate regions under fixed and mobile relay," *IEEE Transactions on Wireless Communications*, vol. 16, no. 12, pp. 8190–8204, 2017.

[18] L. Yuan, S. Bi, S. Zhang, X. Lin, and H. Wang, "Multi-antenna enabled cluster-based cooperation in wireless powered communication networks," *IEEE Access*, vol. 5, pp. 13941–13950, 2017.

[19] S. Boyd and L. Vandenberghe, *Convex Optimization*, Cambridge University Press, 2013.